

**Theory of the diamagnetism above the critical temperature for cuprates**

J. L. González and E. V. L. de Mello

*Departamento de Física, Universidade Federal Fluminense, Niterói, Rio de Janeiro 24210-340, Brazil*

(Received 30 April 2003; revised manuscript received 30 October 2003; published 19 April 2004)

Recently, experiments on high critical temperature superconductors have shown that the doping levels and the superconducting gap are usually not uniform properties but strongly dependent on their positions inside a given sample. Local superconducting regions may develop at the pseudogap temperature  $T^*$  and upon cooling, grow continuously. As one of the consequences a large diamagnetic signal above the superconducting critical temperature  $T_c$  has been measured by different groups. Here we construct a general theory to a disordered superconductor using a critical-state model for the magnetic response to the local superconducting domains between  $T^*$  and  $T_c$  and show that the resulting diamagnetic signal is in agreement with the experimental results.

DOI: 10.1103/PhysRevB.69.134510

PACS number(s): 74.20.-z, 74.25.Ha, 74.72.-h

**I. INTRODUCTION**

There is an increasing interest on the effects of the microscopic intrinsic inhomogeneities in high critical temperature superconductors (HTSC). The fact that these materials have doping level and superconducting gap that, even in some of the best single crystals, vary locally inside a given sample, has profound consequences and a number of unconventional related phenomena are observed<sup>1</sup> specially in the normal region of the HTSC phase diagram. In particular, recent magnetic imaging through a scanning superconducting quantum interference device (SQUID) microscopy has displayed a static local precursor of the Meissner state at temperatures as large as three times the  $T_c$  of an underdoped LSCO (lanthanum strontium copper oxide) film.<sup>2</sup> Following up SQUID magnetization measurements on powder oriented YBCO (yttrium barium copper oxide) and LSCO single crystals<sup>3,4</sup> have shown a rather high magnetic response which, due to its large signal and structure, cannot be attributed solely to the Ginzburg-Landau (GL) theory of fluctuating superconducting magnetization.<sup>5,6</sup> This is an unconventional behavior because low-temperature superconductors exhibit only a much smaller diamagnetic signal above  $T_c$  which is believed to be a consequence of the thermal fluctuations.<sup>7</sup> Therefore such strong magnetic response was interpreted as due to the fluctuating diamagnetism produced by superconducting islands nucleated above  $T_c$ .<sup>3,4,8</sup> On the other hand, the existence of superconducting islands above  $T_c$  is a consequence of a non-uniform or disordered intrinsic carrier density, as pointed out by Ovchinnikov *et al.*<sup>9</sup>

The tendency towards the formation of magnetic domain lines or stripes was predicted long ago<sup>10</sup> and verified experimentally by different groups.<sup>11,12</sup> The stripes are formed by an instability towards charge phase separation which means hole-poor regions of antiferromagnet (AF) insulating separated by hole-rich metallic domains. Recently, the microscopic intrinsic inhomogeneities in the charge distribution, consistent with the presence of charge domains or charge stripes, has been revealed by neutron diffraction.<sup>13</sup> A peak broadening in the atomic pair distribution function was measured and explained by a local microscopic coexistence of doped and undoped materials.<sup>13</sup> Evidences for microscopic

phase separation into normal and superconducting regions were also obtained by muon spin-relaxation rate.<sup>14</sup> Therefore the inclusion of the intrinsic charge inhomogeneities or the tendency of the formation of charge domains in any calculations for the cuprate properties may be far more important than previously anticipated. The main difficulty to incorporate such effect in quantitative calculations is that the exact form of the doping or hole distribution inside a given sample is not exactly known although it is a consensus that the local doping level becomes more uniformly distributed in the materials on crossing from the underdoped into the overdoped region of the phase diagram.<sup>1,13</sup> On the other hand, a considerable improvement in the understanding of the doping level and local superconducting gap functional form has been made by scanning tunneling microscopy/spectroscopy (STM/STS) experiments.<sup>2,15-17</sup>

Based on these findings, we have recently proposed a two-phase model (undoped and doped regimes present in a given compound) described by a bimodal distribution of the holes inside a given compound in order to model the charge distribution for a given compound belonging to a HTSC family.<sup>18</sup> This distribution resembles a typical distribution of a spinodal decomposition of a binary alloy.<sup>19</sup> A two-phase model which arises from the fluctuation phase of the superconducting order parameter was considered previously by Emery *et al.*<sup>20</sup> The basic ideas of our approach are the following: The undoped or hole-poor part of the distribution represents the AF domains and the hole-rich the metallic regions. The width of the metallic distribution decreases with the sample's average doping since, as mentioned above, the hole distribution inside the compounds of a given family become more homogeneous as the average doping level or average charge-density increases.<sup>13</sup> Due to the spatially varying local charge density, it is also expected a distribution of the local  $T_c$ 's, instead of a single and unique value as in usual metallic superconductors. Therefore a given HTSC compound with an average charge density  $n_m$  possesses distributions of the charge density  $n(r)$ , the zero-temperature superconducting gap  $\Delta_0(r)$ , and the superconducting critical temperature  $T_c(r)$ , where the symbol  $(r)$  means a point or small region inside the sample. In this scenario we identify the largest  $T_c(r)$  with the pseudogap temperature  $T^*$  of a given compound.<sup>21</sup> Doping regions with  $n(r) > 0.05$  have a

metallic behavior with a decreasing  $T_c(r)$  following a mean-field pattern.<sup>22</sup> Upon cooling below  $T^*$  the superconducting regions develop at isolated regions [mostly with  $n(r) \leq 0.05$ ] as droplets of rain in the air and eventually they percolate at the sample superconducting critical temperature  $T_c$  at which superconducting long-range order is established. This superconducting percolation scenario for HTSC has also been discussed previously, but with somewhat different approaches, by several authors.<sup>23,24</sup> Therefore, only at or below the percolation temperature  $T_c$  a dissipationless macroscopic electrical or hole current may flow through the sample. Based on these ideas, we have used a bimodal charge distribution in connection with a mean-field calculation to reproduce the phase diagram of  $T^*$  and  $T_c$  as a function of the average doping level for the  $\text{Bi}_2\text{Sr}_2\text{CaCu}_2\text{O}_{8+x}$  and  $\text{La}_{2-x}\text{Sr}_x\text{CuO}_4$  families.<sup>18,25</sup> In these chemical formulas  $x$  is the doping level which is similar to the average charge density, i.e.,  $x = n_m$  for the last (La series) and  $x = 2n_m$  for the former (Bi) family of compounds

The existence of the superconducting regions with different  $T_c$ 's in the material must manifest itself through a number of observable properties: we can number a few such as the pseudogap phenomena, the resistivity, and Hall coefficient temperature dependence, and so on. Here we want to discuss the normal-state magnetization, whose study is the purpose of this paper. Thus, we develop a general theory of the magnetization of an inhomogeneous superconductor which can be applied to the HTSC, in order to explain the recent anomalous magnetization measurements.<sup>3,4</sup> In a similar fashion, Romano<sup>8</sup> introduced a theory for the magnetic response based on the fluctuations in the local order parameter which leads to a Kosterlitz-Thouless transition and the fluctuation-induced diamagnetism<sup>6</sup> of superconducting islands above  $T_c$  which reproduced well the details of the experimental data. Assuming that the superconducting islands started to be formed at  $T^*$ , for measurements at  $T < T^*$  and  $T$  close to but above  $T_c$ , some of these islands must be in a superconducting state and therefore they must yield a local superconducting diamagnetic response. We show below that the measured diamagnetic signal can be understood within this picture of a superconductor formed by static domains with spatially varying  $T_c(r)$ 's. Since the local  $T_c(r)$ 's can be much higher than the sample's superconducting  $T_c$ , we apply the well-known critical-state model (CSM) (Ref. 7) to the magnetization response under an applied field. This approach is valid with the hypothesis of the measured temperature to be below that of the irreversibility line of the local superconducting regions. Some kink of hysteretic behavior was observed in YBCO and in LSCO samples<sup>3,4</sup> indicating that the irreversible temperature is above  $T_c$ . We demonstrate here that this simple procedure is able to explain and reproduce the main features of the precursor diamagnetism measured behavior.

## II. THE MODEL

From the above discussion, since the hole distribution is not uniform, we can think of a HTSC sample as formed by different metallic and insulating regions of a few nanometers

of magnitude. As a consequence of such distribution, at a given temperature above  $T^*$  there are insulating and metallic regions below  $T^*$  there are insulating, metallic, and superconducting regions which started to condensate in the metallic regions at  $T^*$ ; and below  $T_c$  the long-range superconducting order is achieved by a percolation transition while there still are some metallic and insulating regions present in the sample. As in Ref. 18, we model these insulator and metallic regions by a bimodal  $\gamma$  type distribution with parameters which are based on the STM/STS analysis<sup>16</sup> and which was used to derive the HTSC phase diagrams.

Now we want to use the above ideas to discuss the magnetic response  $M(B)$  of such inhomogeneous superconductors to an external magnetic field, between  $T_c$  and  $T^*$ . In this range of temperature, it is clear that only the superconducting regions or droplets with their  $T_c(r)$ 's bigger than  $T_c$  contribute to the diamagnetic sample's magnetization. These superconducting regions contribute to the sample's magnetization with a diamagnetic signal which depends on  $B$  and the overall sample's magnetization will be the sum of all these contributions.

In order to estimate  $M(B)$  we follow the ideas and the procedures of the CSM to each superconducting droplet. Upon applying an external magnetic field, a critical current  $J_c$  is established which opposes the field as  $J_c(B) = \alpha(T)/B$  according to Ohmer *et al.*<sup>26</sup>  $\alpha(T)$  is a temperature-dependent local constant which we have taken to be proportional to  $[T_c(n(r)) - T]$ . Hereafter we call the hole local density  $n(r)$  of a given domain of  $n$  and the whole sample's average density of  $n_m$ . For simplicity we take these superconducting droplets as cylinders of radius  $R$ , which is sufficiently small, in order to have a constant charge density  $n$  and consequently the critical temperature  $T_c(n)$  is the same within such cylinder region. (As the temperature decreases, more droplets appear and the superconducting regions increase by aggregation of droplets of different  $n$ .) The CSM approach leads to the magnetic-field dependence of the magnetization in each small cylinder as<sup>26</sup>

$$M_1(B) = -\frac{B}{\mu_0} \quad \text{for } B \leq B_{c1}, \quad (1)$$

$$M_2(B) = -\frac{B}{\mu_0} + \frac{4B^3}{5\mu_0 B^{*2}} - \frac{8B^5}{15\mu_0 B^{*4}}, \quad B_{c1} \leq B \leq B^*, \quad (2)$$

$$M_3(B) = -\frac{B}{\mu_0} - \frac{4B^*}{15\mu_0} \left( 2\frac{B^5}{B^{*5}} - 5\frac{B^3}{B^{*3}} - 2 \left[ \frac{B^2}{B^{*2}} - 1 \right]^{5/2} \right) \quad \text{for } B^* \leq B \leq B_{c2}. \quad (3)$$

In the last expression,  $B^*$  is the value of the applied external field which produce full penetration inside a cylindrical superconducting droplet, and it depends on its size as  $B^* = \sqrt{2\alpha(T)\mu_0}R$ .  $\mu_0$  is the vacuum permmissivity. The dependence of the local critical temperatures  $T_c(n)$  is taken to

be that of the pseudogap temperature of a given compound with its average charge density, namely,  $T^*(n_m)$ . Thus,  $T_c(n)$  is a function which has its maximum at  $n=0.05$  and decreases monotonously, that is, we take the local superconducting critical temperatures as a linear function of  $n$ ,  $T_c(n)=T_0-b(n-n_c)$ .  $T_0$  is the highest pseudogap temperature near the onset of superconductivity, i.e.,  $n_c=0.05$ , and  $b$  is chosen in order to wave  $T_c(0.3)=0$ . Notice that, since  $T_c(n)$  is a linear decreasing function of  $n$ , the droplets with lower values of  $n$  (just above  $n_c$ ) are more robust to an applied field in the sense that its superconducting state is not easily destroyed by the external field.

Since  $T_c(n)$  is constant inside a superconducting cylindrical droplet, the critical fields ( $B_{c1}$  and  $B_{c2}$ ) inside the droplets will have their temperature dependence given by the GL theory, e.g.,  $B_{c1}(T)=B_{c1}(0)[1-T/T_c(n)]$  and  $B_{c2}(T)=B_{c2}(0)[1-T/T_c(n)]$ . Taking into account the dependence of  $T_c(n)$  on  $n$ , we arrive at the expressions for the critical fields  $B_{c1}(T,n)$  and  $B_{c2}(T,n)$ . A similar functional form is supposed for  $B^*$  due to the  $\alpha(T)$  temperature dependence. Thus,

$$B_{c1}(T,n)=B_{c1}(0)\left[1-\frac{T}{T_0-b(n-n_c)}\right], \quad (4)$$

$$B_{c2}(T,n)=B_{c2}(0)\left[1-\frac{T}{T_0-b(n-n_c)}\right], \quad (5)$$

$$B^*(T,n)=B^*(0)\left[1-\frac{T}{T_0-b(n-n_c)}\right]. \quad (6)$$

When a given sample is submitted to an applied external magnetic field  $B$ , the superconducting droplets with carrier concentration  $n$  for which the applied field is higher than their second critical field  $B_{c2}(T,n)=B_{c2}(0)(1-T/[T_0-b(n-n_c)])$ , do not contribute to the sample magnetization. This condition is verified for droplets with  $n>n_{max}$ , where  $n_{max}(B_{c2})=n_c+T_0/b-(T/b)/[1-B/B_{c2}(0)]$  is obtained inverting Eq. (5). Since  $T_c(n)$  is a decreasing function of  $n$ , only the droplets with  $n$  bigger than  $n_{max}$  do not contribute to the sample's magnetization because their superconductivity is destroyed by the field  $B$ . Thus we expect that

$$M(T,B)=\int_{n_c}^{n_{max}(B_{c2})} P(n)M(B,T,n)dn. \quad (7)$$

Where  $P(n)$  is the distribution function for the local hole doping level at the many clusters inside a given HTSC inferred in Ref. 18. However, in the context of the CSM, depending on the intensity of the applied field, there are different possibilities in which each domain contributes to  $M(B)$ . In the low-field regime the superconducting clusters will contribute to the magnetization of the sample in three forms: there are some clusters, which are not penetrated by the field  $B$ , that is  $B\leq B_{c1}(T,n)$  and they contribute to the magnetization with perfect diamagnetism [Eq. (1)]. These clusters have their carrier concentration in the interval,  $n<n_c+T_0/b-(T/b)/[1-B/B_{c1}(0)]$ . The second group of clus-

ters have their  $B_{c1}(T,n)$  lower than the applied field but  $B$  is also lower than  $B^*(n,T)$ . This group is partially penetrated by the field and they contribute to  $M(B)$  according to Eq. (2). These domains have their carrier concentration in the interval  $n_c+T_0/b-(T/b)/[1-B/B_{c1}(0)]<n<n_c+T_0/b-(T/b)/[1-B/B^*(0)]$ . Finally, there are some superconducting granules for which the applied field is higher than  $B^*(T,n)$  but also lower than  $B_{c2}(T,n)$ . These domains contribute to the magnetization according to Eq. (3). Therefore, for a sufficient by low applied field, the general expression for  $M(B)$  is given by

$$\begin{aligned} M(T,B) &= \int_{nm}^{n_{max}(B_{c1})} P(n)M_1(B,T,n)dn \\ &+ \int_{n_{max}(B_{c1})}^{n_{max}(B^*)} P(n)M_2(B,T,n)dn \\ &+ \int_{n_{max}(B^*)}^{n_{max}(B_{c2})} P(n)M_3(B,T,n)dn. \quad (8) \end{aligned}$$

Upon increasing the applied field the number of droplets that are not penetrated by the field decreases and for fields higher than  $B_{c1}(n_m,T)$  there are not any granules contributing with perfect diamagnetism. Notice that  $B_{c1}(n_m,T)$  is the maximum first critical field that a superconducting region can achieve. For  $B\geq B_{c1}(n_m,T)$ , all the droplets are partially or totally penetrated by the field and they contribute to the sample's magnetization according Eqs. (1)–(3):

$$\begin{aligned} M(T,B) &= \int_{nm}^{n_{max}(B^*)} P(n)M_2(B,T,n)dn \\ &+ \int_{n_{max}(B^*)}^{n_{max}(B_{c2})} P(n)M_3(B,T,n)dn. \quad (9) \end{aligned}$$

Finally for fields higher than  $B^*(0)(1-T/[T_0-b(n_m-n_c)])$ , all the superconducting granules of the sample are totally penetrated by the field and their contribution to the magnetization is

$$M(T,B)=\int_{nm}^{n_{max}(B_{c2})} P(n)M_3(B,T,n)dn. \quad (10)$$

These last three equations express the total  $M(B)$  for any value of the applied field.

In order to obtain a reliable value of  $M(B)$  and to compare with the experimental results, we have incorporated the fluctuation magnetizations induced by the superconducting order parameter, an effect which should be always present, regardless of whether the superconductor is more or less inhomogeneous. As noted in Ref. 27, for superconducting droplets with a homogeneous order parameter and with dimensions  $d$  approximately equal to the coherent length  $\xi(T)$ , the Ginzburg-Landau model provides an exact solution for  $M_{fluct}(B)$ . Here we use a simplified ‘‘zero dimensional’’ for superconducting clusters of radius  $d$  smaller or near the coherence length  $\xi(T)$ , namely,<sup>3</sup>

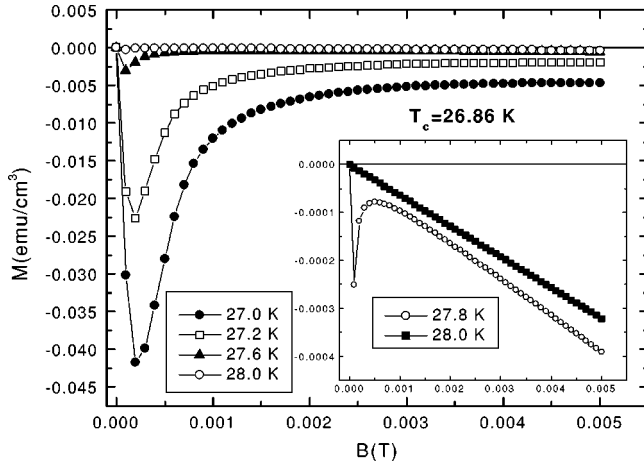


FIG. 1. Magnetization for parameters appropriated to the overdoped LSCO as calculated from Eqs. (7)–(11). The inset shows the change in the magnetization behavior as the anomalous contribution vanishes when the temperature is increased. This result is to be compared with the measurements from Ref. 4.

$$M_{fluct}(T, B) = -\frac{2/5k_B(\pi\xi Td)^2B}{\Phi_0^2(T/T_c - 1) + (\pi\xi Bd)^2/5}, \quad (11)$$

where  $k_B$  is the Boltzmann constant,  $\Phi_0$  is the quantum flux, and  $d \approx \xi \propto (T - T_c)/T_c$ . This last expression yields a linear  $M_{fluct}(B)$  dependence for low fields and it has been incorporated in our calculations. The specific results for  $M_{fluct}$  are shown in the insets of Figs. 1 and 2.

Therefore Eqs. (7)–(11) furnish the complete  $M(B, T)$  curve for a HTSC at temperatures  $T^* > T > T_c$ . Our numerical results will be compared with the experimental results in the following section.

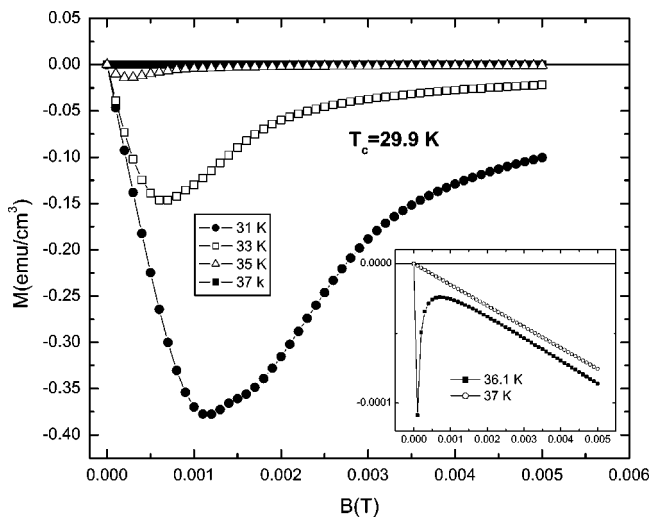


FIG. 2. Magnetization for parameters appropriated to the underdoped LSCO as calculated from Eqs. (7)–(11). The inset shows the change in the magnetization behavior as the anomalous contribution vanishes when the temperature is increased. This result is to be compared with the measurements from Ref. 4.

### III. RESULTS AND DISCUSSION

The above theory was developed to model the measured magnetization curves of the  $\text{La}_{1-x}\text{Sr}_x\text{CuO}_4$  family of compounds. The major difficulty is that the measurements of the pseudogap temperature curve for any family seems to vary depending on the technique used.<sup>21</sup> In fact there are differences even in the  $T_c$  measured values for the same HTSC compound when reported by different groups, but such differences are small compared with those for the  $T^*$  measurements.

In the calculations we used values taken from the local precursor diamagnetic signal<sup>2</sup> and Nernst effect<sup>28</sup> measurements which display some local precursor order near  $T \approx 100$  K. This value is considerably lower than the values of  $T^*$  from transport measurements.<sup>21</sup> A possible explanation for this discrepancy is that the transport measurements detect the onset of pair formation while for the magnetic response a large density of pairs must be present in order to display a measurable local response. Thus, we have taken  $T_0 = 80$  K,  $b = 320$  K for the carrier concentration linear dependence of the droplet's critical temperature  $T_c(n)$ . In fact  $T_c(n)$  is not necessarily linear but this is an approximation which fits reasonably well with the experimental data but which may be improved in the future as new experimental data becomes available. The antiferromagnetic cutoff for the carrier concentration is  $n_c = 0.05$  and the superconducting cutoff is  $n_m = 0.3$ . The probability  $P(n)$  is also not well known but some of its features were inferred from STM measurements and the phase diagram, as discussed in Ref. 18.

In Fig. 1 we plot the results of our model with the parameter which corresponds to a  $n_m = 0.2$ . According to our model this concentration corresponds to a LSCO overdoped sample with a critical temperature of  $T_c = 26.86$  K. In the calculations we have used  $B_{c1}(0) = 0.01$  T,  $B_{c2}(0) = 20$  T, and  $B^*(0) = 0.025$  T. The value of  $B_{c2}$  is derived from experimental values.<sup>29</sup> The values of  $B_{c1}(0)$  and  $B^*(0)$  are not found in the literature, however, one can make a fair estimation of the ratio  $B_{c2}/B_{c1}$  through the GL parameter  $\kappa$  which is about 100 for some YBCO and LSCO compounds.<sup>30</sup> The inset shows that for  $T = 27.8$  K there is a low contribution at low fields from the superconducting island in the sample while at high fields only a linear contribution comes from the diamagnetic fluctuation signal. At  $T = 28$  K there is no more contribution from the superconducting droplets and all the diamagnetic signals are only due to the magnetization fluctuations. Note that  $T = 28$  K is the most weak diamagnetic signal which appears in Fig. 1. The inset demonstrates that, at these temperatures or above, only the fluctuating magnetization is important.

The qualitative features of the measurements are entirely reproduced and are simply explained by our model; at low fields the perfect diamagnetism is expected for droplets for which the fields are lower than their  $B_{c1}$ . We expect  $B_{c1}$  to be weak because the superconducting regions formed above  $T_c$  are small and isolated. By the same token, the droplets penetrating field  $B^*$  should not be very strong which decreases rapidly the overall diamagnetic signal for field much weaker than  $B_{c2}$ . As the applied field increases, the magnetic

response dies off and is reduced to the fluctuations. This is the reason why  $M(B)$  has a minimum at very low applied fields. In Fig. 1 we show this upturn field near  $B_{up} = 0.0001$  T which agrees with the experimental values.<sup>4</sup> It is worthwhile to mention that previous estimation for the upturn field considering only the Lawrence-Doniach fluctuations<sup>5</sup> in a layered superconductor<sup>3</sup> yields expected values near  $B_{up} = 10$  T. These figures bring out the importance of the CSM applied to the superconducting islands above  $T_c$  to explain the experimental results.

In order to study the effect of the local charge inhomogeneities, we have also performed similar calculations with parameters appropriate to an underdoped compound. It is well known that, within the same family, overdoped samples have a more homogeneous charge distribution than the underdoped ones.<sup>13</sup> Thus, we have chosen a compound with almost the same critical temperature  $T_c$  than that of the overdoped sample (shown in Fig. 1) to single out the effect of the charge inhomogeneities. In this simulation we used a carrier concentration of average concentration of 0.11 with its appropriate distribution  $P(n)$  and with a critical temperature of 29.9 K. We have chosen the same field parameters, e.g.,  $B_{c1}(0) = 0.01$  T,  $B_{c2}(0) = 20$  T, and  $B^*(0) = 0.025$  T. The results from our simulations are shown in Fig. 2. In this case the overall diamagnetic signal persists for measurement temperatures higher than those for the overdoped sample. The  $B_{up}$  field is dislocated to higher values but it is still much lower than the homogeneous Lawrence-Doniach<sup>5</sup> fluctuating field. This is a consequence of the fact that an underdoped sample has a more inhomogeneous charge distribution than the overdoped compounds possessing regions which the field easily penetrates (with local  $n \approx 0.25$ ) and others where are more robust to field penetration (with local  $n \approx 0.1$ , for instance). This fact is taken into account through the distribution parameters used in our simulation. The results for an underdoped compound are shown in Fig. 2 which can be also noticed in the inset that as the temperature approaches 37 K, the diamagnetic contribution of the superconducting droplets decreases and for measurements of temperature higher than  $\approx 37$  K there is only the fluctuations contribution.

It is important to mention that, although our calculations are very much in qualitative agreement with the magnetic imaging results<sup>2</sup> and with the powder oriented SQUID magnetic measurements,<sup>3,4</sup> there are other experiments which have not detected a  $B_{up}$  field<sup>31</sup> and have interpreted their results as solely due to the GL fluctuating diamagnetic theory.<sup>6</sup> However, an inspection of their curves indicates that they have not looked in detail at the low-field region. The absence of a  $B_{up}$  field was also found on an optimally doped powder oriented YBCO compound<sup>3</sup> whose curves followed the pure fluctuating magnetic response. In this case, the pos-

sible interpretation for a pure fluctuating diamagnetism signal, according to our theory, is that these samples must have a very good degree of charge homogeneity. This interpretation can be experimentally tested because these compounds must have  $T^*$  almost equal or equal to  $T_c$ , as may be the case.<sup>21</sup>

Another point which hinders a good quantitative agreement with the experimental results is that the technique used seems also to be very important in probing the details of the magnetization above  $T_c$ ; while the scanning microscopy results on a LSCO film indicate the presence of a visible diamagnetic signal at temperatures as large as three times the sample's  $T_c$ ,<sup>2</sup> the SQUID magnetization measurements detected a diamagnetic signal on oriented powder only around 10% above  $T_c$ .<sup>3,4</sup>

It is important to emphasize that, in our calculations of  $M(B, T)$ , the islands that contribute to the diamagnetic signal are in the critical state, and the measured temperature  $T$  is below their local  $T_c(r)$ . On the other hand, the Romano's calculations yield an upturn field which is almost independent of the temperature while in Fig. 2 we can see clearly that it decreases with the applied temperature. Future experiments may distinguish which mechanism is more important or if some compounds exhibit one type and others exhibit the other.

#### IV. CONCLUSION

We have constructed a general theory of the diamagnetism applicable to a disordered superconductor with a distribution of regions with different local superconducting  $T_c$ 's. We have shown that the procedure reproduces the qualitative features of the unusual diamagnetic signal above  $T_c$  measured for several HTSC samples. This was done applying a CSM and the well-known magnetic effects for fields between  $B_{c1}$  and  $B_{c2}$  to the superconducting regions formed at temperatures below  $T^*$  of an inhomogeneous HTSC compound. The quantitative results can be improved when experiments provide better estimates of  $T^*$  and  $B_{c1}$ .

Our results demonstrated that, as concluded also from other different calculations,<sup>4,8</sup> the measured normal-state magnetization curves, the  $B_{up}$  fields, and the STM magnetic imaging results may be interpreted through the formation of static superconducting islands at temperatures above the sample's  $T_c$ .

#### ACKNOWLEDGMENTS

We want to thank Professor A. Rigamonti for discussions that led to this work and for providing us with the experimental results prior to their publications. Partial financial aid from CNPq and FAPERJ is gratefully acknowledged.

<sup>1</sup>T. Egami and S.J.L. Billinge, in *Physical Properties of High-Temperatures Superconductors V*, edited by D.M. Ginsberg (World Scientific, Singapore, 1996), p. 265.

<sup>2</sup>I. Iguchi, I. Yamaguchi, and A. Sugimoto, *Nature (London)* **412**,

420 (2001).

<sup>3</sup>A. Lascialfari, A. Rigamonti, L. Romano, P. Tedesco, A. Varlamov, and D. Embriaco, *Phys. Rev. B* **65**, 144523 (2002).

<sup>4</sup>A. Lascialfari, A. Rigamonti, L. Romano, A. Varlamov, and I.

- Zucca, Phys. Rev. B **68** 100505(R) (2003).
- <sup>5</sup>C. Baraduc, A. Buzdin, J-Y. Henry, J-P. Brison, and L. Puech, Physica C **248**, 138 (1995).
- <sup>6</sup>A. Sewer and H. Beck, Phys. Rev. B **64**, 014510 (2001).
- <sup>7</sup>Michael Tinkham, *Introduction to Superconductivity* (McGraw-Hill, New York, 1975).
- <sup>8</sup>L. Romano, Int. J. Mod. Phys. B **17**, 423 (2003).
- <sup>9</sup>Yu.N. Ovchinnikov, S.A. Wolf, and V.Z. Kresin, Phys. Rev. B **60**, 4329 (1999).
- <sup>10</sup>J. Zaanen and O. Gunnarson, Phys. Rev. B **40**, 7391 (1989).
- <sup>11</sup>J.M. Tranquada, B.J. Sternlieb, J.D. Axe, Y. Nakamura, and S. Uchida, Nature (London) **375**, 561 (1995).
- <sup>12</sup>A. Bianconi, N.L. Saini, A. Lanzara, M. Missori, T. Rosseti, H. Oyanagi, Y. Yamaguchi, K. Oda, and T. Ito, Phys. Rev. Lett. **76**, 3412 (1996).
- <sup>13</sup>E.S. Bozin, G.H. Kwei, H. Takagi, and S.J.L. Billinge, Phys. Rev. Lett. **84**, 5856 (2000).
- <sup>14</sup>Y.J. Uemura, Solid State Commun. **126**, 23 (2003).
- <sup>15</sup>C. Howald, P. Fournier, and A. Kapitulnik, Phys. Rev. B **64**, 100504 (2001).
- <sup>16</sup>S.H. Pan, J.P. O'Neal, R.L. Badzey, C. Chamon, H. Ding, J.R. Engelbrecht, Z. Wang, H. Eisaki, S. Uchida, A.K. Gupta, K.W. Ng, E.W. Hudson, K.M. Lang, and J.C. Davis, Nature (London) **413**, 282 (2001).
- <sup>17</sup>K.M. Lang, V. Madhavan, J.E. Hoffman, E.W. Hudson, H. Eisaki, S. Uchida, and J.C. Davis, Nature (London) **415**, 412 (2002).
- <sup>18</sup>E.V.L. de Mello, E.S. Caixeiro, and J.L. González, Phys. Rev. B **67**, 024502 (2003).
- <sup>19</sup>John W. Cahn, Acta Metall. **9**, 795 (1961).
- <sup>20</sup>V.J. Emery, S.A. Kivelson, and J.M. Tranquada, Proc. Natl. Acad. Sci. U.S.A. **96**, 8814 (1999).
- <sup>21</sup>T. Timusk and B. Statt, Rep. Prog. Phys. **62**, 61 (1999).
- <sup>22</sup>V.J. Emery and S.A. Kivelson, Nature (London) **374**, 434 (1995).
- <sup>23</sup>Yu.N. Ovchinnikov, S.A. Wolf, and V.Z. Kresin, Phys. Rev. B **63**, 064524 (2001); Physica C **341-348**, 103 (2000).
- <sup>24</sup>D. Mihailovic, V.V. Kabanov, and K.A. Müller, Europhys. Lett. **57**, 254 (2002).
- <sup>25</sup>E.V.L. de Mello, M.T.D. Orlando, E.S. Caixeiro, J.L. González, and E. Baggio-Saitovich, Phys. Rev. B **66**, 092504 (2002).
- <sup>26</sup>M.C. Ohmer and J.P. Heinrich, J. Appl. Phys. **44**, 1804 (1973).
- <sup>27</sup>J.P. Gollub, M.R. Beasley, R. Callarotti, and M. Tinkham, Phys. Rev. B **7**, 3039 (1973).
- <sup>28</sup>Z.A. Xu, N.P. Ong, Y. Wang, T. Kakeshita, and S. Uchida, Nature (London) **406**, 486 (2000); cond-mat/0108242 (unpublished).
- <sup>29</sup>Y. Ando, G.S. Boebinger, A. Passner, L.F. Schneemeyer, T. Kimura, M. Okuya, S. Watauchi, J. Shimoyama, K. Kishio, K. Tamasaku, N. Ichikawa, and S. Uchida, Phys. Rev. B **60**, 12 475 (1999).
- <sup>30</sup>C.P. Poole, Jr., H.A. Farach, and R.J. Creswick, *Superconductivity* (Academic Press, London, 1995), p. 271.
- <sup>31</sup>Carlos Carballeira, Jesus Mosqueira, A. Revcolevschi, and Felix Vidal, Phys. Rev. Lett. **84**, 3157 (2000).